J Mater Sci (2010) 45:987–992
DOI 10.1007/s10853-009-4029-z

An unusual morphology and crystallization behavior in in situ formed polyphenylene oxide/polyamide 6 blends

Yulin Li · Guisheng Yang

Received: 2 August 2009 / Accepted: 9 November 2009 / Published online: 17 November 2009

Abstract Novel polyphenylene oxide/polyamide 6 (PPO/PA6) blends were synthesized via in situ polymerization of ε-caprolactam with PPO dissolved in it. The introduction of 10 wt% PPO into PPO/PA6 led to phase inversion of the blends, which was nearly completed by incorporating 15 wt% PPO into the blends. A single crystallization temperature (T_c) of PA6 was detected for PPO/PA6 with 1–4 wt% PPO, while double T_c existed in the blends with 6–15 wt% PPO. After eliminating previous thermal history, PPO/PA6 containing no more than 6 wt% PPO gave a single melting point (T_m), but the blends with 10–15 wt% PPO exhibited double T_m. Increasing PPO content in PA6 resulted in the transformation of its crystal form from α-crystal to γ-crystal, which might be attributed to hindrance of crystallization of PA6 particles in PPO-rich phase.

Introduction

Great interests have been attracted to polymer blends of PA6 and PPO from industrial and academic point of view because the combination of PPO and PA6 has a chance to give mutually complementary properties [1]. The disadvantages of PA6, such as low heat distortion temperature and poor dimensional stability can be complemented by high-dimensional and good thermal properties of PPO, while the deficiencies of PPO, such as poor solvent resistance and difficulty to process can be improved by incorporating PA6. Though, much attention has been paid to the morphology and mechanical properties of PPO/PA6, few were reported on the structure effects, especially the crystallization behavior and crystalline structure [2].

Polyamide 6 exhibited polymorphism structures that contained two types of stable crystal form: monoclinic α-form and pseudo-hexagonal γ-form [3–6], which are very sensitive to the way of preparing samples. The α-form crystal of PA6 can be obtained by slow cooling from the melt state [7]. Usually, γ-form crystal is an unstable form. The γ-form crystal of PA6 can be transformed into the α-form crystal by annealing PA6 [8], by drawing and then by annealing PA6 [9], or by treating PA6 with a phenol aqueous solution [10]. Reversely, the α-form of PA6 can be transformed to the γ-form by treating PA6 with iodine [5, 11], incorporating clay into PA6 [12–17].

In our previous studies [18], a series of PA6 molecular composites with PA66 were synthesized via in situ anionic polymerization of ε-caprolactam (CL) with soluble in it PA66. It was found that PA66 macromolecules can be inserted, disposed in molecular level, into PA6 matrix by this method. It was because of the strong hydrogen bonding interactions in the mixture that PA66 did not crystallize and phase separated out during in situ polymerization process. PA66 macromolecules dispersed in a molecular level in PA6 interfered with the arranging order of hydrogen bonding of PA6, changed its crystalline structure, and reduced its crystallization rate and crystallinity.

Similar to the approach to synthesize PA66/PA6 molecular composites, the blends of polyphenylene oxide/polyamide 6 (PPO/PA6) with a quite high glass temperature, which does not form strong hydrogen bonding with

Y. Li (✉)
Centro de Química da Madeira, Universidade da Madeira, Campus da Penteada, 9000-390 Funchal, Portugal
e-mail: yulin@iccas.ac.cn

Y. Li · G. Yang
Joint Laboratory of Polymer Science and Materials, Institute of Chemistry, Chinese Academy of Sciences, Beijing 100080, People's Republic of China

PA6, have been synthesized via in situ anionic ring opening polymerization of CL with PPO dissolved in it, instead of PA66. It was found that incorporating a small content of PPO (1–3 wt%) also improved the impact strength and the elongation of PA6 with maintenance of its tensile strength, which may be related to the special morphology and crystal structure in the in situ formed PPO/PA6 blends [19].

What would happen when more amount of PPO was incorporated into PA6 via in situ polymerization of CL? The purpose of this contribution is to further investigate the effect of an PPO in a broader range (0–15 wt%) on the morphology of PPO/PA6 blends, crystallization behavior, and crystal structure of PA6 using scanning electron microscopy (SEM), differential scanning calorimetry (DSC), and wide-angle X-ray diffraction (WAXD), respectively. Interestingly, it was found that a variation of PPO led to a dramatic change in the morphology and an unusual crystallization behavior and crystal transformation of PA6 in the resulting PPO/PA6 blends.

Experimental section

Materials

Polyphenylene oxide (PPO) was obtained from General Electric, (Commercial Grade, BHPP 820). ε-Caprolactam was bought from Nanjing Oriental Chemical Company, (Commercial Grade, Jiangsu province, P.R. China). Sodium hydrate (NaOH) and toluene diisocyanate (TDI) were purchased from Shanghai Chemical Reagents Company, (Analysis Grade, P.R. China), and they were used without further purification.

Preparation of PPO/PA6 composite

PPO was dissolved in molten ε-caprolactam monomer at 180 °C under nitrogen atmosphere, and a homogeneous transparent polymer–monomer solution was observed. It was vacuumed at 170 °C for about 20 min to remove water. Then 0.2 wt% NaOH was added under stirring and continuously vacuumed for another 10 min. After 0.4 wt% TDI was added with stirring, the mixture was then immediately poured into a mold preheated to 180 °C, and polymerized in oven at 180 °C for 20 min. After polymerization, the products were cooled to room temperature and extracted with boiling water to eliminate the residual monomer for 10 h. Then, the extracted products were dried at 80 °C in oven. The obtained PPO/PA6 blends with different PPO contents were designated as "PPO/PA6" below for short.

Measurements

The impact-fractured surfaces of specimen images were observed on a JSM-6360LV scanning electron microscope (SEM). Surfaces of fracture specimens were gold-sputtered before observation.

DSC was carried out on a Perkin–Elmer Pyris-7 differential scanning calorimeter (DSC) calibrated with indium. DSC scans were performed with Perkin–Elmer aluminum DSC pans and covers that were sealed with a Volatile Sealer Assembly. All the DSC measurements were performed from room temperature to 250 °C at a heating rate of 10 °C/min under nitrogen atmosphere, and stayed there for 10 min to eliminate previous thermal history for all samples.

Wide angle X-ray diffraction (WAXD) analysis was performed on a Rigaku D/Max-III X-ray diffraction(XRD) analyzer equipped with a rotating anode generator system using CuK_{α} ($\lambda = 1.54$ Å) radiation at an operating current of 25 mA and a voltage of 35 kV. The scanning rate was 1°/min.

Results and discussion

Figure 1 shows the SEM morphologies of cryo-fractured surface of PPO/PA6 with PPO content no more than 4 wt%. Small particles of PPO were dispersed in PA6 matrix for PPO/PA6 with 1–3 wt% PPO (Fig. 1a–f). For PPO/PA6 with 4 wt% PPO, dispersed PPO-rich particles with the spherical inclusions of PA6 were found, besides the appearance of PPO particles with larger size (Fig. 1g, h). The size of the particles obviously increased with increasing amounts of PPO.

Compared to PPO/PA6 with 4 wt% PPO, the addition of 5 wt% PPO into PA6 increased the number of PA6-included PPO particles in the blend (Fig. 2a), although there was no obvious increase in the particle size. The incorporation of 6 wt% PPO caused a drastic increase in the size of PPO-rich particles. The introduction of 10 wt% PPO into PPO/PA6 led to phase inversion between PPO and PA6, and the phase inversion was nearly finished for the blends with 15 wt% PPO.

Figure 3 shows the DSC curves of PPO/PA6 blends with different PPO contents. It can be seen that a single crystallization peak (T_c) was observed for PPO/PA6 with less than 6 wt% PPO, while two T_c peaks were detected in the blends containing 6–15 wt% PPO. Compared to pure PA6, T_c of PA6 in PPO/PA6 with 1–10 wt% PPO decreased with increasing PPO content. The decrease of T_c together with the appearance of second low T_c in the blends with 6–15 wt% PPO indicated that the presence of PPO in PPO/PA6 restricted the crystallization of PA6. However, the high T_c of PPO/PA6 with 15 wt% of PPO was about 4 °C

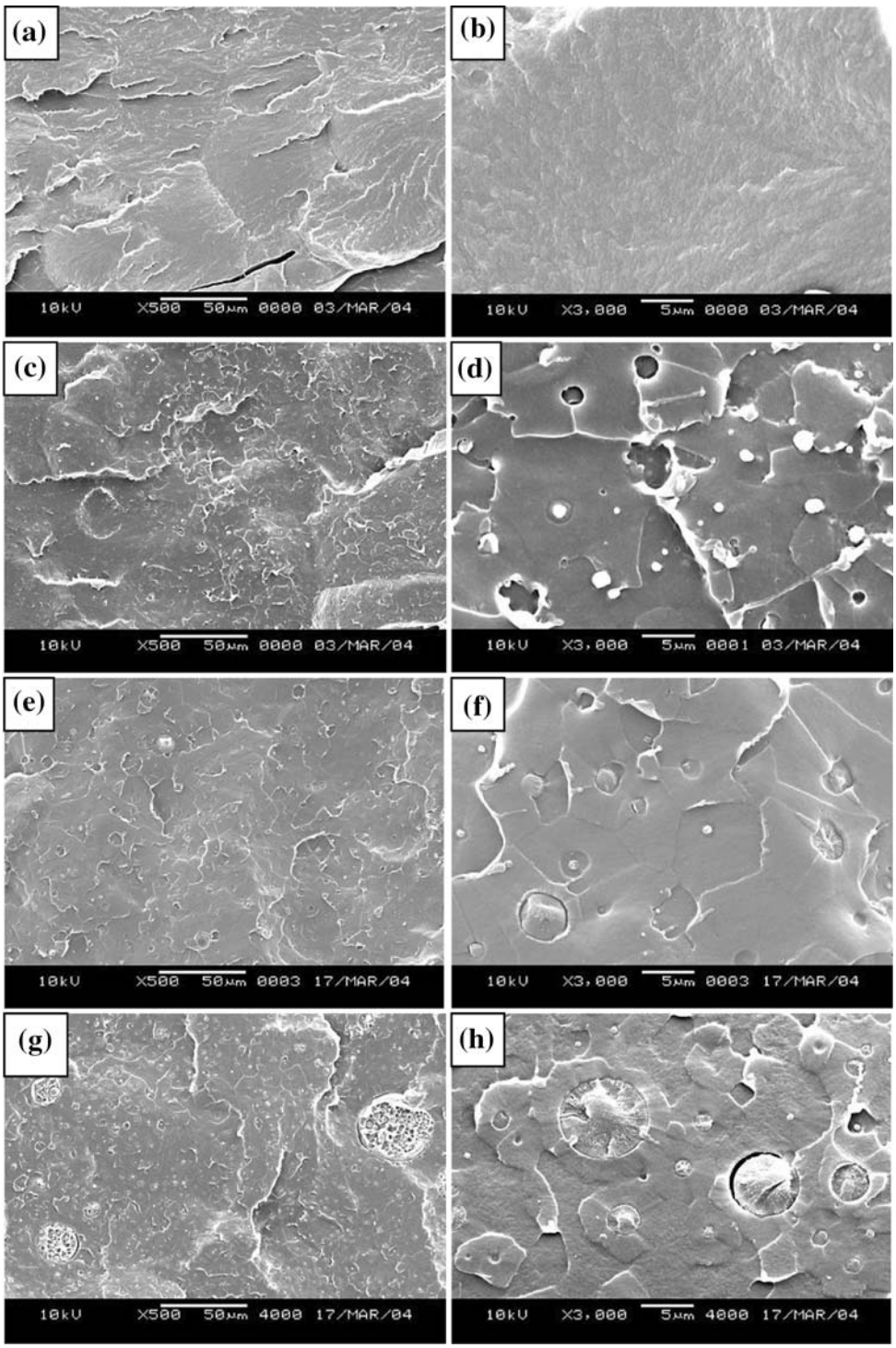

Fig. 1 SEM micrographs of fractured surfaces of PPO/PA6 containing **a**, **b** 0 wt% PPO; **c**, **d** 1 wt% PPO; **e**, **f** 3 wt% PPO; **g**, **h** 4 wt% PPO

higher than that of pure PA6, which suggested that PPO might act as nucleating agent to increase crystallization rate of PA6 [2, 20–22]. The changes of T_c of PA6 in the blend may depend on the balance of nucleation and hindrance of PPO on PA6.

During the first scanning, the DSC melting curves of PPO/PA6 containing different PPO had melting peaks with different shapes (Fig. 4), which suggested the quite complicated melting behaviors due to the effect of the thermal history during in situ polymerization process.

To eliminate the effect of thermal history, the samples were kept at 250 °C for 10 min and then the second scanning was performed for PA6 and its blends with PPO. The DSC melting curves shown in Fig. 5 indicated that PPO/PA6 containing PPO/PA6 with 1–6 wt% PPO had a single melting peak (about 220 °C), while the blends with 10–15 wt%

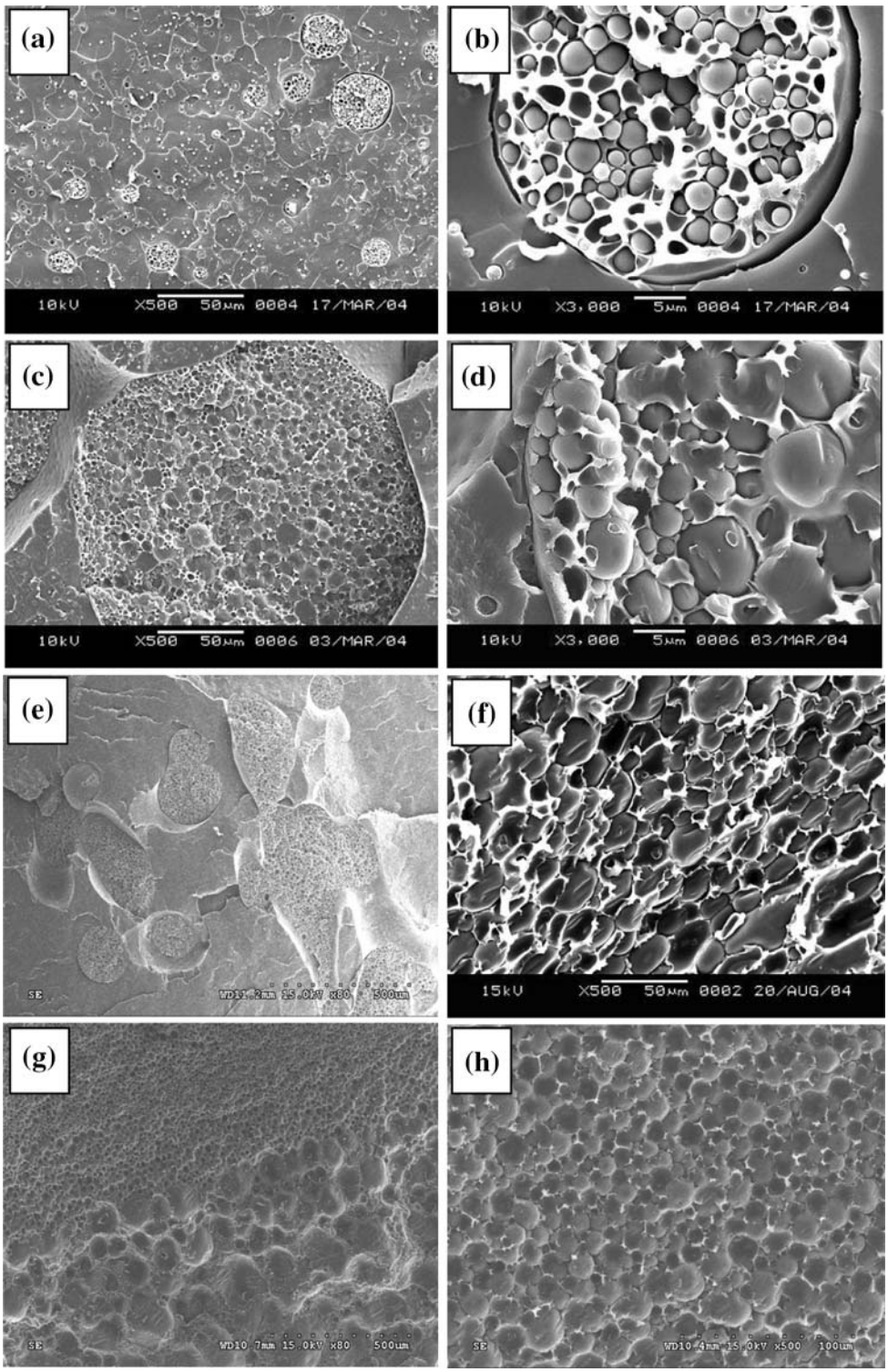

Fig. 2 SEM micrographs of fractured surfaces of PPO/PA6 containing **a**, **b** 5 wt% PPO; **c**, **d** 6 wt% PPO; **e**, **f** 10 wt% PPO; **g**, **h** 15 wt% PPO

PPO exhibited double peaks. Interestingly, the high T_m of PPO/PA6 with 15 wt% PPO was 1 °C higher than that of pure PA6, while the high T_m of the PPO/PA6 with 10 wt% PPO was 1 °C less than that of PA6. The increase of PA6 in the blends did not cause the depression of T_m of PA6 (higher T_m for the blends with higher PPO content), which indicates that the two components are immiscible [23]. The appearance of the lower T_c and T_m might ascribe to the restricted crystallization of the PA6 particles dispersed in PPO and the melting of the restricted crystallites, respectively, because PPO had a quite high glass-transition temperature (T_g = 221 °C, as shown in Fig. 5j).

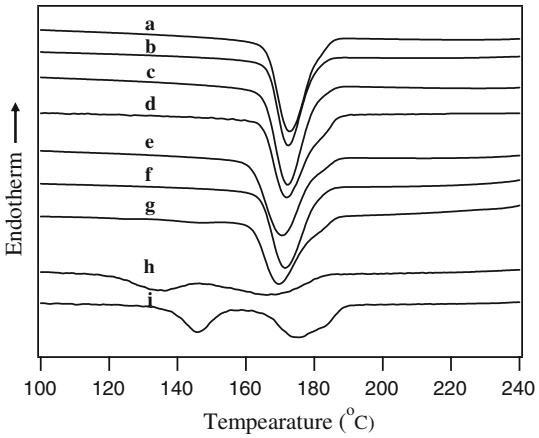

Fig. 3 DSC crystallization curves of PPO/PA6 containing PPO: (a) 0 wt% PPO; (b) 1 wt% PPO; (c) 2 wt% PPO; (d) 3 wt% PPO; (e) 4 wt% PPO; (f) 5 wt% PPO; (g) 6 wt% PPO; (h) 10 wt% PPO; (i) 15 wt% PPO

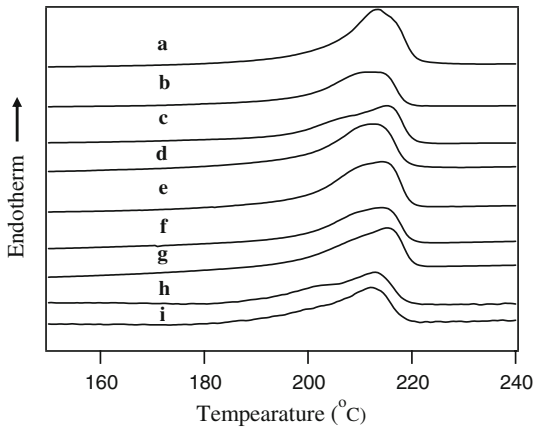

Fig. 4 First scanning DSC melting curves of PPO/PA6 containing PPO: (a) 0 wt% PPO; (b) 1 wt% PPO; (c) 2 wt% PPO; (d) 3 wt% PPO; (e) 4 wt% PPO; (f) 5 wt% PPO; (g) 6 wt% PPO; (h) 10 wt% PPO; (i) 15 wt% PPO

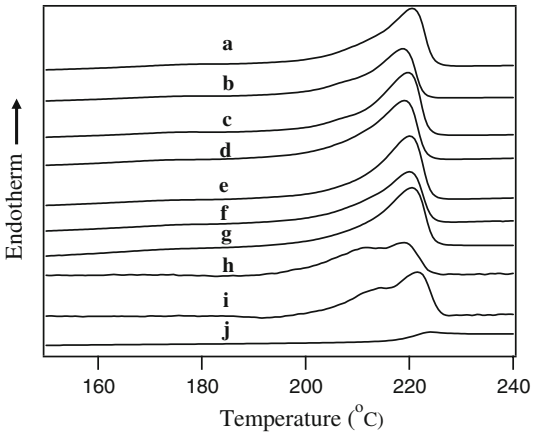

Fig. 5 Second scanning DSC melting curves of PPO/PA6 containing PPO after eliminating thermal history by keeping samples at 250 °C for 10 min: (a) 0 wt% PPO; (b) 1 wt% PPO; (c) 2 wt% PPO; (d) 3 wt% PPO; (e) 4 wt% PPO; (f) 5 wt% PPO; (g) 6 wt% PPO; (h) 10 wt% PPO; (i) 15 wt% PPO and (j) pure PPO

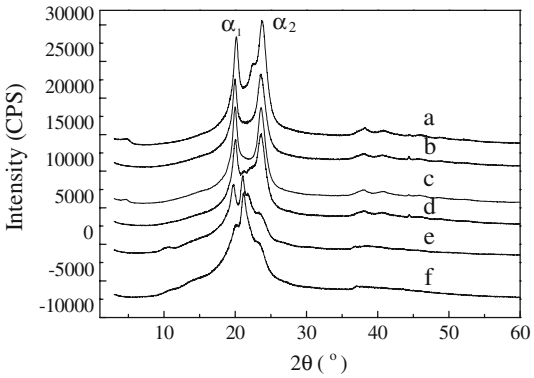

Fig. 6 WAXD intensity profile of PPO/PA6 containing PPO (a) 0 wt% PPO; (b) 3 wt% PPO; (c) 5 wt% PPO; (d) 6 wt% PPO; (e) 10 wt% PPO; (f) 15 wt% PPO

Figure 6 presents the WAXD intensity profile of PPO/PA6 with different PPO content. The WAXD patterns of PPO/PA6 reveal that the peaks of α-crystal form of PA6 decreased with the increase of PPO, and α-crystal form diminished and nearly disappeared when the amount of PPO was increased to 15 wt%. At the same time, the peaks of γ-crystal form apparently increased with incorporation of more than 10 wt% PPO. This indicates that the presence of PPO induced the transition of α crystal form to γ-crystal form of PA6 in PPO/PA6. The α_1 peak arises from the distance between hydrogen-bonded chains, and the α_2 peak reflects the separation of the hydrogen-bonded sheets [7, 24]. The increase of the *d*-spacing of the α_1 peak could be attributed to the thermal expansion of the lattice, while the change in the *d*-spacing of the α_2 peak might be related to respective lattice distortion (shown in Table 1). The above results reveal that the presence of PPO significantly influenced the crystalline structure. We assume that the rigid molecular motion of PPO around PA6 dispersed particles restricts the adjustment of conformation of PA6 macromolecular chains, limiting the formation of hydrogen-bonded sheets of α-phase, which can be verified by the transformation of α-crystal form to γ-crystal form of PA6 by increasing PPO content in PPO/PA6.

Thermodynamics, kinetics, and polymerization rates are competing factors that control the phase separation of in situ polymerization system during the process of polymerization of reactive solvent. It is easier for thermoplastic/ε-caprolactam systems via in situ polymerization to manipulate morphological structure than common thermoplastic/thermosetting system, due to its faster reaction rate of the former than that of the latter [25–27].

Table 1 Effect of PPO content on *d*-spacing (*d*) of α-crystal form of PA6 in PPO/PA6 blends

PPO content (wt%)	0	3	5	6	10	15
d_1 (nm)	0.4397	0.4436	0.4436	0.4427	0.4480	0.4423
d_2 (nm)	0.3732	0.3764	0.3764	0.3757	0.3792	–

Secondary phase separation may take place in reaction-induced phase separation, which results in dispersed particles with inclusion of the continuous phase matrix [28]. The secondary phase-separation process occurs when the blend first passed into the metastable region and then into the unstable region such that some nucleation and growth precede spinodal decomposition, or the composition of the coexisting phases changes due to continuous polymerization of the reactive monomers such that they themselves become unstable [29].

The poor miscibility between PA6 and PPO made PPO phase segregate in the early stage of curing, during which the PPO-rich phase formed due to the relatively low viscosity of the blends. Then the further phase separation occurred just in the separated phases. The diffusion between PA6-rich phase and PPO-rich phase would be hindered by the increase of viscosity of the system, due to the quite high T_g of PPO, the relatively low polymerization temperature and quick polymerization rate of ε-caprolactam. As a consequence, the individual PPO-rich phase appeared with the introduction of more than 3 wt% PPO, and the phase inversion would happen with further increasing PPO content in the blends. The crystallization behavior of the dispersed particles of PA6 was restricted by the rigid molecular motion of PPO matrix around PA6 particles. The restricted crystallization behavior led to the transition of α-crystal form to γ- crystal form of PA6 in PPO/PA6 with increasing PPO.

Conclusions

Polyphenylene oxide/polyamide 6 (PPO/PA6) blends were prepared via in situ polymerization of ε-caprolactam in the presence of PPO. The introduction of 10 wt% PPO into PA6 caused phase inversion between PPO and PA6, which was nearly finished by incorporating 15 wt% PPO into the blends. PPO/PA6 containing less than 1–4 wt% PPO exhibited a single T_c, while the blends with 6–15 wt% PPO gave double T_c. After eliminating thermal history, PPO/PA6 containing no more than 6 wt% PPO gave a single melting point (T_m), but double T_m existed in the blends with 10–15 wt% PPO. The incorporation of PPO induced the transformation of α-crystal form of PA6 to γ-crystal, which might be attributed to the restricted crystallization of PA6 particles in PPO-rich phase.

References

1. Chiang CR, Chang FC (1996) J Appl Polym Sci 61:2411
2. Chiang CR, Chang FC (1998) J Polym Sci Polym Phys 36:1805
3. Holmes DR, Bunn CW, Smith DJ (1955) J Polym Sci 17:159
4. Donald C, Vogelsong DC (1963) J Polym Sci Part A 1:1055
5. Arimoto H (1964) J Polym Sci Part A 2:2283
6. Arimoto H, Ishibashi M, Hirai M (1965) J Polym Sci Part A 3:317
7. Murthy NS, Curran SA, Aharoni SM, Minor H (1991) Macromolecules 24:3215
8. Gurato G, Fichera A, Grandi FZ, Zanetti R, Canal P (1974) Makromol Chem 175:953
9. Ho JC, Wei KH (2000) Macromolecules 33:5181
10. Maillo J, Pages P, Vallejo E, Lacorte T, Gacén J (2005) Euro Polym J 41:753
11. Kinoshita Y (1959) Makromol Chem 33:1
12. Tjong SC (2006) Mat Sci Eng R Rep 53:73
13. Mathias L, Davis R, Jarrett W (1999) Macromolecules 32:7958
14. Winberg P, Eldrup M, Pedersen NJ, van Es MA, Maurer FHJ (2005) Polymer 46:8239
15. Kim G, Michler GH, Ania F, Calleja FJB (2007) Polymer 48:4814
16. Li T, Ma J, Wang M, Tjiu WC, Liu T, Huang WJ (2007) J Appl Polym Sci 103:1191
17. Karaman VM, Privalko VP, Privalko EG, Lehmann B, Friedrich K (2005) Macromol Symp 221:85
18. Li Y, Yang G (2004) Macromol Rap Commun 25:1714
19. Li Y, Xie T, Yang G (2006) J Appl Polym Sci 99:2076
20. Liang B, Pan LJ (1994) J Appl Polym Sci 54:1945
21. Menyhárd A, Varga J, Liber A, Belina G (2005) Eur Polym J 41:669
22. Menyhárd A, Varga J (2006) Eur Polym J 42:3257
23. Nishi T, Wang TT (1975) Macromolecules 8:909
24. Ramesh C (1999) Macromolecules 32:3721
25. Parnell S, Min K (2005) Polymer 46:3649
26. Cui J, Yu Y, Chen W, Li S (1997) Macromol Chem Phys 198:3267
27. Li Y, Xie T, Yang G (2006) J Appl Polym Sci 99:335
28. Williams RJJ, Rozenberg BA, Pascault JP (1997) Adv Polym Sci 128:95
29. Henderson IC, Clarke N (2004) Macromolecules 37:1952